ISSN 1070-3632, Russian Journal of General Chemistry, 2015, Vol. 85, No. 6, pp. 1565–1574. © Pleiades Publishing, Ltd., 2015.
Original Russian Text © R.Yu. Yakovlev, A.S. Osipova, A.S. Solomatin, I.I. Kulakova, G.P. Murav'eva, N.V. Avramenko, N.B. Leonidov, G.V. Lisichkin, 2013, published in Rossiiskii Khimicheskii Zhurnal, 2013, Vol. 57, No. 5, pp. 86–96.

An Approach to Unification of the Physicochemical Properties of Commercial Detonation Nanodiamonds

R. Yu. Yakovlev[a], A. S. Osipova[b], A. S. Solomatin[a,b], I. I. Kulakova[b], G. P. Murav'eva[b], N. V. Avramenko[b], N. B. Leonidov[a], and G. V. Lisichkin[b]

[a] *Pavlov Ryazan State Medical University, ul. Vysokovol'tnaya 9, Ryazan, 390026 Russia*
e-mail: yarules@yandex.ru; n.leonidov@yandex.ru

[b] *Lomonosov Moscow State University, Moscow, 119991 Russia*
e-mail: kulakova@petrol.chem.msu.ru; muravieva@kge.msu.ru; natali@td.chem.msu.ru; lisich@petrol.chem.msu.ru

Received February 1, 2013

Abstract—In recent years, detonation nanodiamond is regarded as a promising material for biomedical applications. However, a significant problem that stops of intensive development of this area is a absence of commercial NDs standardization. This article presents the results of the study of physicochemical properties of several industrial nanodiamonds available in the international market. The differences of physicochemical characteristics of nanodiamonds produced, selected and purified in various ways are shown. A method is developed for industrial processing of nanodiamonds, that represents high-temperature hydrogenation of diamond surface and allows to unify their properties. It is shown that after these processing nanodiamonds have the same surface chemistry and can form stable hydrosols. The proposed method of industrial nanodiamonds unification can become a universal method of its standardization.

Keywords: Detonation nanodiamond, physicochemical properties, unification, standardization, hydrogenation, surface chemistry, hydrosols

DOI: 10.1134/S1070363215060365

INTRODUCTION

Ultradispersed detonation diamonds, or detonation nanodiamonds, with their unique physicochemical properties, compare favorably with other carbon nanomaterials, which makes them attractive for diversified applications in science and technology, including biology and medicine [1]. One of the promising applications of nanodiamonds is that of a carrier for drug delivery systems in nanomedicine [2, 3].

Nanodiamonds are synthesized by detonation of a mixture of explosives with a negative oxygen balance (e.g., an octogen–trotyl or hexogen–trotyl mixture, 40–70 wt %) in a blast chamber filled with an inert medium (coolant). This procedure yields a large number of nanometer-sized diamond nuclei within ca. 0.3 μs [4]. It was found [1] that the use of an aqueous solution of a reducing agent as the armor for the charge allows producing higher-quality nanodiamonds.

The synthesis product is a detonation diamond-containing carbon, or the so-called diamond-containing blend, which is, essentially, a complex physicochemical system containing both diamond carbon and various graphite-like and other carbon structures. Diamond-structured particles are fairly small, several nanometers in size; they occur within aggregated nondiamond carbon particles. The product synthesized can be more correctly characterized as a cluster material with a complex hierarchy of the levels of aggregation of diamond and nondiamond forms of carbon, with specific forms of relaxation of energy-saturated surfaces. The excess surface energy of nanodiamonds is compensated by the surface functional groups containing heteroatoms (N, H, O, etc.) [5, 6].

Today, no single optimal technology exists for synthesis, purification, and dispersion of detonation nanodiamonds, as well as no established system of their certification [7]. Different producers follow different technical specifications in preparation of detonation nanodiamonds, which affects the physicochemical parameters of their synthesis and purification

Table 1. Characteristics of the nanodiamond samples. Data available from nanodiamonds producers

Characteristic	Value
Sample I: PL-D-G01, PlasmaChem, Germany	
Product form	Powder
Specific surface area, $m^2 g^{-1}$	350–390
Coherent scattering region size, nm	4
Size of the diamond aggregates, nm	5–15
Ash content, %	<1.4
Sample II: Standart ND, Adamas Nanotechnologies, USA	
Density, g cm^3	3.5
Solubility	Insoluble
Conditions for formation of stable suspensions	pH=4–5 (10 % aqueous suspension)
Sample III: PL-SDND, PlasmaChem, Germany	
Product form	Powder
Diamond crystal size, nm	4–6
Impurity content, %	Fe < 0.3, Cu < 0.01, Zn < 0.01, Mn < 0.01, Si + Cr + Ca + Ti < 0.01
Ash content, %	<1.4
Pycnometric density, g cm^3	3.18
ζ-Potential, mV (conditions for formation of stable aqueous	–55±5
Sample IV: UDA-TAN, Tekhnolog Special Design and Technological Bureau, Russia	
Chemical purification	Nitric acid, ammonolysis at 200°C under pressure
Drying method	Spray drying
Aggregates	Small, unstable
Nondiamond carbon content, wt%	1.1
Incombustible impurities, wt%	0.85

processes. The latter determine the amount and composition of the impurities and the chemical state of the surface of the diamond nanoparticles and their ability for deaggregation and formation of stable hydrosols, as well as the behavior of the nanoparticles in chemical modification reactions [8]. This often leads to nonreproducibility and instability of the physicochemical characteristics of not only commercial nanodiamonds of different brands but also of those from different batches of the same brand. Moreover, it is not always possible to reproduce published results of nanodiamonds studies, because the brand and the characteristics of the nanodiamonds are often not provided in publications.

The criteria to be met by commercially produced detonation nanodiamonds intended for development of drug delivery systems are as high as those posed on drugs. Efficient use of nanodiamonds for biomedical applications requires unification of standard characteristics.

In this connection, a comprehensive study of the properties of commercial nanodiamonds of various brands with the aim of identification of the differences and unification of their properties is essential. Here, we carried out a comparative study of the physicochemical properties of nanodiamonds available from different producers and suggested ways to unify them in order that identical physicochemical properties of the nanodiamond surface and the possibility of formation of stable suspensions therefrom be ensured.

EXPERIMENTAL

Objects. We studied four brands of nanodiamonds available from different producers: PL-D-G01, PlasmaChem, Germany (sample I), Standart ND, Adamas Nanotechnologies, USA (sample II), PL-SDND, PlasmaChem, Germany (sample III), and UDA-TAN, Tekhnolog Special Design and Technological Bureau, Russia (sample IV).

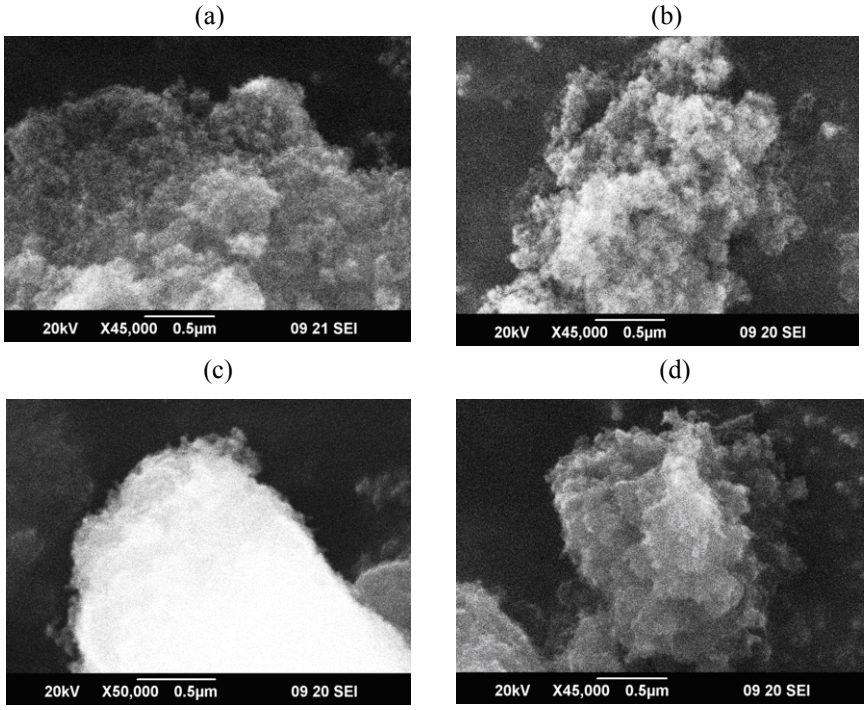

Fig. 1. Microphotographs of the nanodiamond samples: (a) sample I, (b) sample II, (c) sample III, and (d) sample IV. Scanning electron microscopy.

The initial characteristics of the samples are presented in Table 1. However, these data do not allow comparison of the samples, since the certificates of the commercial nanodiamonds contain only selected and fairly different characteristics.

Preparation of nanodiamond hydrosol. Deagregation of all the nanodiamond samples was carried out under identical conditions. Nanodiamond suspensions were prepared with the use of an MEF91 sonicator (MELFIZ, Russia) (frequency 22 kHz, ultrasonic power 250 W cm^{-2}, power output 20–30%) and a TsLn-16 centrifuge (Changsha Xiangzhi Centrifuge Instrument Co., China) (at 11000 rpm, 12000 g). To obtain suspensions, 500 mg of the nanodiamond powder were added to 25 mL of distilled water and subjected to several ultrasonication (1 min)–centrifugation (6000 g) cycles.

Physico-chemical research methods. The electron-microscopic images of the nanodiamond samples were obtained on a LEO 1455 VP (Carl Zeiss, Germany) scanning electron microscope equipped with a Centaurus detector and on a JEM-2100 F (JEOL, Japan) ultrahigh-resolution transmission electron microscope with point-to-point resolution of 2 Å and lattice resolution of 1 Å.

The FTIR spectra of the samples were recorded on an IR200 Thermo Nicolet (Thermo Scientific, USA) Fourier-transform infrared spectrometer (resolution 2 cm^{-1}, 50 scans) using KBr pellets. For preparation of pellets, a weighted portion (0.80 mg) of the nanodiamond was mixed with a KBr powder pre-dried in a vacuum (140.0 mg), after which 75.0 mg the resulting mixture of nanodiamond together with the matrix was taken and pressed. The absorption bands were assigned on the basis of the data from [9, 10].

The chemical composition of the sample surface was analyzed by X-ray photoelectron spectroscopy (XPS) on a LAS-3000 (Riber, France) instrument equipped with an OPX-150 hemispherical analyzer using nonmonochromatic AlK_α radiation (1486.6 eV) from an aluminum anode at the tube voltage of 12 kV and emission current of 20 mA. The carbon C1*s* line with the binding energy of 285 eV served for calibration. The working chamber was evacuated to the residual pressure of 7×10^{-8} Pa with the use of an ion pump.

The thermochemical properties of the initial nanodiamond were studied by differential scanning calorimetry on a Mettler DSC-30 (Mettler Toledo, USA) calorimeter in the temperature range from –80 to +30°C. A weighted portion (~20 mg) of the

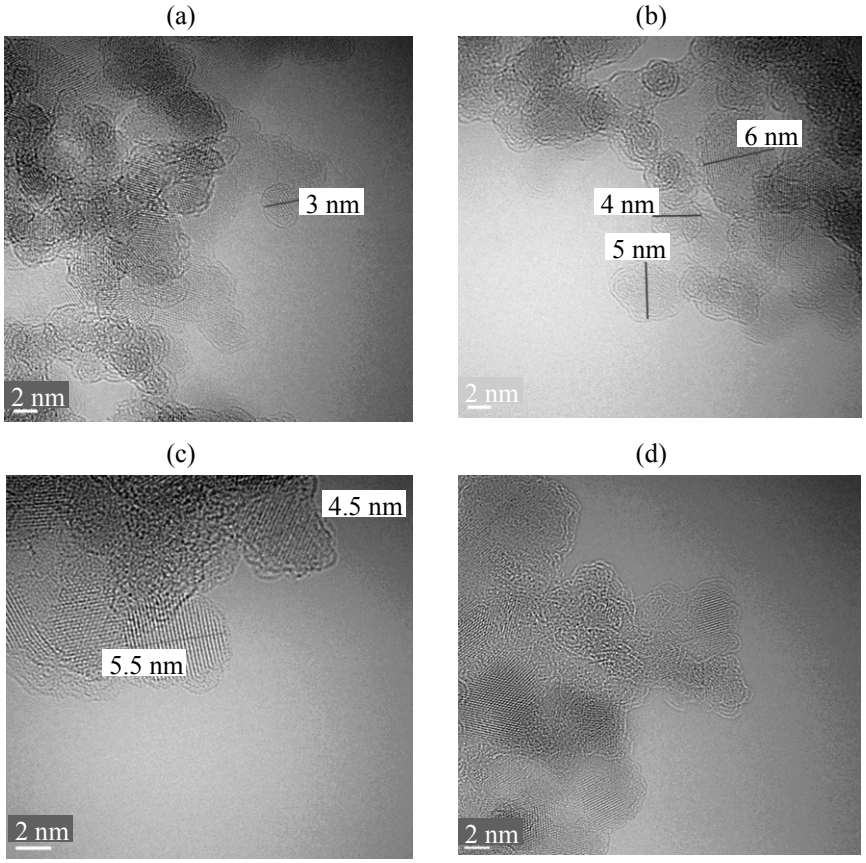

Fig. 2. Microphotographs of the nanodiamond particles of samples (a, b) III and (c, d) IV. Transmission electron microscopy.

nanodiamond sample was placed into a ~50-mg aluminum crucible preliminarily weighed on a Mettler TG50 thermobalance. Next, a small amount of water was added into the crucible, after which the latter was hermetically sealed and weighed once again; the mass of the water added was estimated from the mass difference. The resulting paste was cooled with liquid nitrogen to the temperature of –80°C and then heated at a constant rate of 5°C min^{-1} to 30°C.

The nanodiamond size and ζ-potential were measured by the dynamic light scattering technique on a Zetasizer Nano ZS Zen3600 (Malvern Instruments, UK) instrument. Prior to measurements, the samples of the hydrosol of the nanodiamond were ultrasonicated.

The X-ray diffraction analysis of the nanodiamond powder samples was carried out on a STOE STADI P (STOE & Cie, Germany) diffractometer in θ/θ geometry with CuK_α radiation. The average size of the coherent scattering region of the nanodiamond was determined by the approximation technique based on analysis of the integral width of the (111) and (200) diffraction peaks which were recorded at the step size of 0.05° and step time of 50 s at each point. The size of the coherent scattering region was calculated by the Scherrer formula.

RESULTS AND DISCUSSION

The difference in the structure of nanoparticle aggregates in the powders can be a significant factor affecting the properties of nanodiamonds of different brands. A scanning electron microscopic examination (Fig. 1) showed that all the samples have an ultramicrostructure and contain loose aggregates of different sizes. Sample III was slightly different structurally from the remaining samples; also, it was strongly overexposed in the micrograph (Fig. 1c). This may be due to a high content of oxygen-containing groups formed during preparation of the sample because, as known, it is isolated from a diamond-containing blend by chemical dispersion via multistage

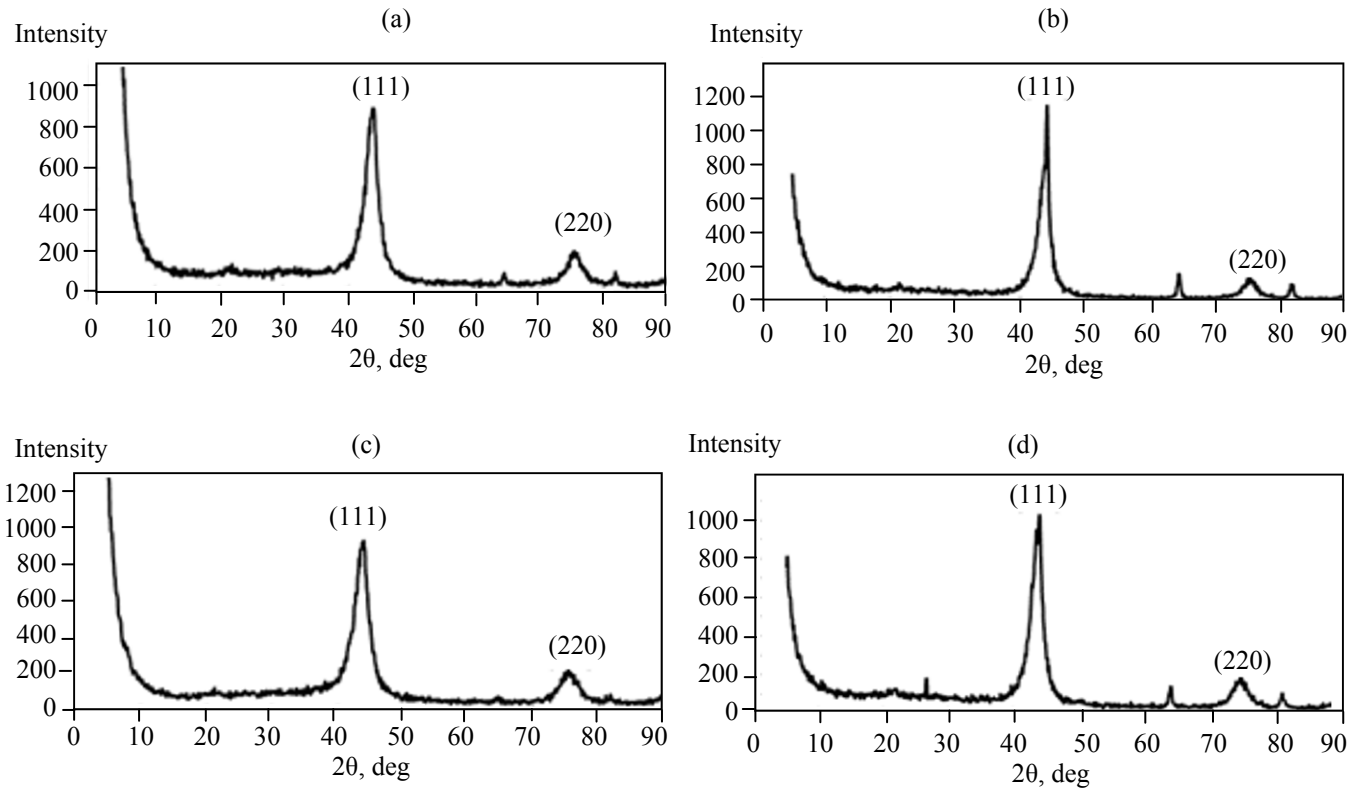

Fig. 3. X-ray diffraction patterns of the initial nanodiamond samples: (a) sample I, (b) sample II, (c) sample III, and (d) sample IV.

treatment with strong acids (using catalyst), followed by exhaustive treatment to remove cations and anions by chromatography and electrophoresis techniques.

Figure 2 shows the microphotographs of samples III and IV, obtained by high-resolution transmission electron microscopic technique; the images of the particles of the two remaining samples are identical to those presented in Fig. 2. It is seen that the particles are spherically-shaped, with the size ranging mostly from 3 to 10 nm; the particles in sample III proved to be generally smaller than those in the other three samples.

The X-ray diffraction patterns of all the samples (Fig. 3) contain reflections corresponding to the (111) and (220) diamond crystal faces. Broadening of the reflections in the diffraction patterns indicates that all the nanodiamond samples have a small the coherent scattering region (CSR). Although the shapes of the curves of the experimental (111) and (220) reflections are asymmetric, the average size of the CSR was estimated for all the samples, specifically at 4.19, 4.62, 3.91, and 4.35 nm for samples I, II, III, and IV, respectively.

The degree of aggregation of the nanodiamond particles in the powders was estimated by the differential scanning calorimetry technique [11, 12] which allows detecting thermal effects at melting of the ice nanophase in the inter-particle spaces in the nanodiamond aggregates. The thermograms (Fig. 4) show that sample III is the most deaggregated one: Only this sample exhibits a clearly noticeable peak at a temperature near –7°C corresponding to melting of nanoscale ice crystals in the pores of the aggregates. The degree of aggregation proved to be the highest for sample II.

It can assume that nanodiamonds in biology and medicine, mainly, will be applied in the form of a stable hydrosol [13, 14]. It is known that the ability of nanodiamonds to form colloidal solutions is influenced by the surface state, size, and ζ-potential of the particles. Therefore, it seems essential that the particle size and hydrosol stability for samples of different brands be estimated and optimal conditions for the hydrosol formation be selected.

It was established previously [15] that, for a nanodiamond suspension subjected to ultrasonication followed by centrifugation, the degree of dispersion tends to increase with increasing number of the treatment cycles.

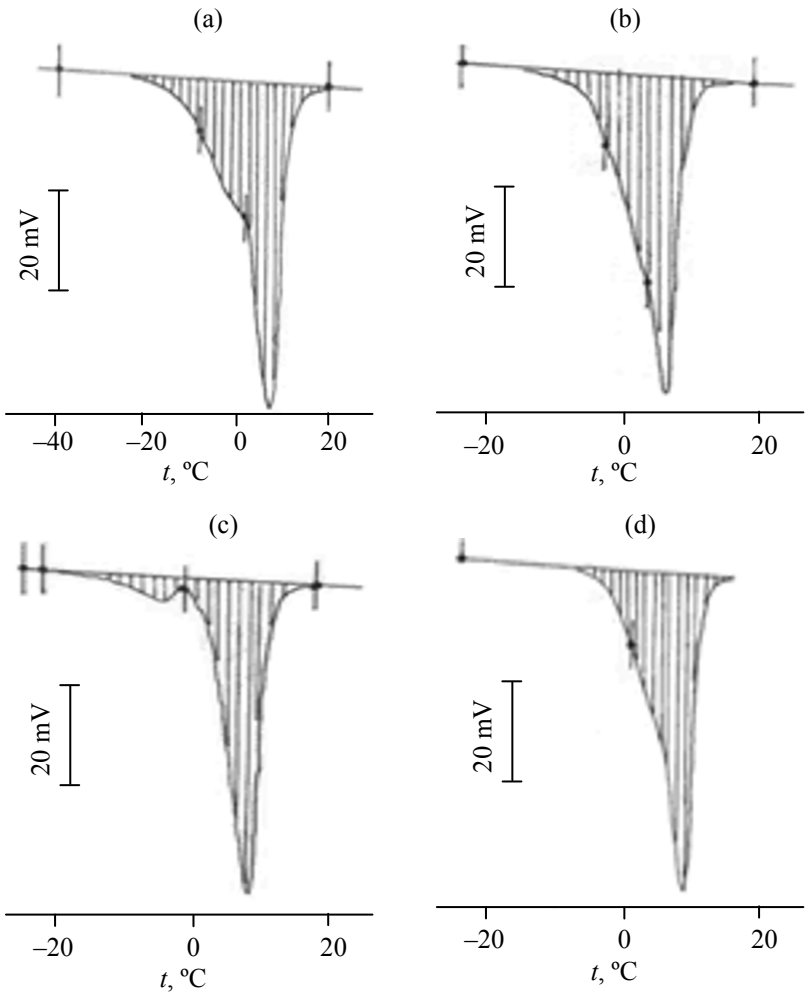

Fig. 4. Differential scanning calorimetry curves for the initial nanodiamonds: (a) sample I, (b) sample II, (c) sample III, and (d) sample IV.

We carried out intercomparison of the characteristics of aqueous suspensions obtained from the tested samples under identical conditions. To this end, we prepared 2% aqueous suspensions of the initial nanodiamonds.

Table 2. Characteristics of the nanodiamond hydrosols after nine treatment (ultrasonication + centrifugation) cycles

Sample no.	Particle size[a], nm		ζ-Potential of the particles, mV	
	initial sample	hydrogenated sample	initial sample	hydrogenated sample
I	600±50	50±10	–4.2±3.0	+45±3
II	550±50	50±10	–10.6±4.5	+40±4
III	50±50	45±10	–41.6±10.5	+41±5
IV	60±10	50±10	+33.8±4.5	+45±12

[a] Maximum in the distribution curve.

These suspensions were subjected to nine cycles of ultrasonication (2 min) followed by centrifugation (5 min, 6000 g). For the resulting suspensions, the dynamic light scattering spectra were recorded, and the particle size and ζ-potential were determined (Table 2). It is seen from Table 2 that the hydrosols prepared from the initial powders of nanodiamonds of different brands strongly differ both in the particle size and ζ-potential. Only for samples III and IV we obtained fairly stable hydrosols characterized by small sizes of the aggregates and high ζ-potentials. Obviously, these findings can be associated with the differences in the chemical state of the diamond particle surface.

Analysis of the FTIR spectra of the nanodiamond samples (Fig. 5) revealed the following features. All the spectra do not contain absorption bands in the 2600–1850 cm^{-1} region, associated with vibrations of the crystal lattice of diamond. The most obvious

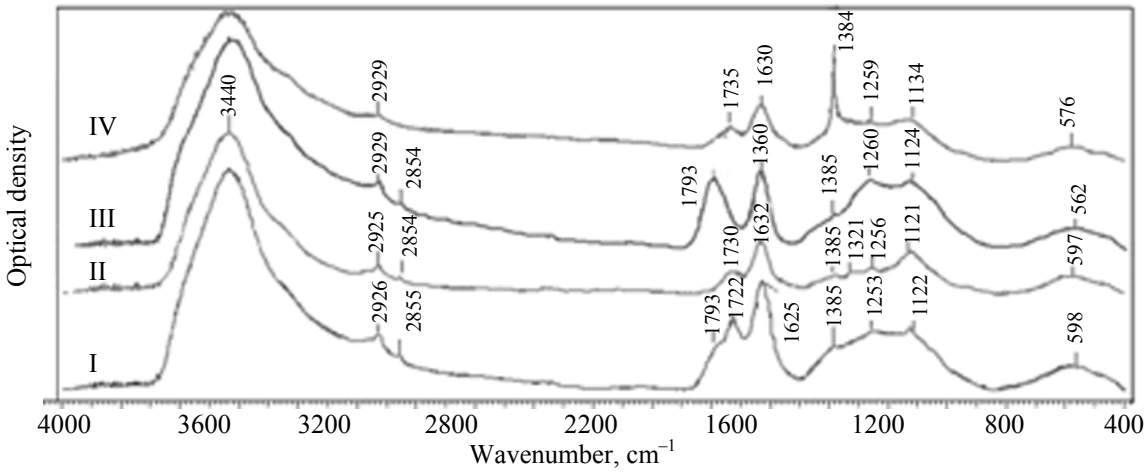

Fig. 5. FTIR absorption spectra of the initial nanodiamond samples.

reason lies in a high concentration of the surface functional groups and their higher absorption coefficients compared to the C–C bonds.

The spectra of all the samples contain absorption bands with maxima at 3440 and 1630 cm^{-1}. The former band is very broad and asymmetric and has a complex structure due, apparently, to strongly pronounced vibrations of the associated hydroxy groups on the nanodiamond surface and in adsorbed water. The latter band is fairly narrow and symmetric; it is associated with bending vibrations of the adsorbed water molecules and partly overlaps with the neighbor band corresponding to the carbonyl group vibrations.

In the 2850–2950 cm^{-1} region there are absorption bands corresponding to the C–H vibrations involving the sp^3 hybridized carbon atom. It is recognized that the band at 2926 cm^{-1} corresponds to the C–H group on the octahedral face of diamond, and the band at 2854 cm^{-1}, to that on the cubic face [16].

The 1720–1790 cm^{-1} region provided the most comprehensive information for identification of the differences between the nanodiamond samples tested. The spectra of samples I and III contain an absorption band with the maximum at 1790 cm^{-1} which was assigned to the carbonyl in the bridging groups

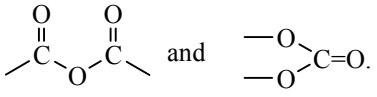

This band was not observed in the spectra of samples II and IV, but they contain a band with the maximum at 1730 cm^{-1} corresponding to absorption of carbonyl group. However, the latter is also part of carboxy, ester, and aldehyde groups, which complicates assignment of the absorption bands in the spectral region considered.

In the 1000–1500 cm^{-1} region the spectra of the samples tested differ substantially. Identification of the bands is complicated by absorption of numerous organic groups and, furthermore, by the intrinsic absorption of the diamond lattice [17] in this region, which leads to strong overlapping of the bands. The structureless absorption bands with poorly resolved peaks, observed in the 400–1000 cm^{-1} region, are similar for all the samples and provide little information regarding the samples.

By contrast to samples I, II, and III, sample IV exhibits a narrow intense FTIR absorption band at 1384 cm^{-1} corresponding to absorption of the nitrate ion. A possible reason for appearance of this band is washing of the sample with nitric acid.

Table 3. Elemental composition of the surface layers of the nanodiamond particles. XPS data

Sample no.	Element content, at % (normalized with respect to the C, O, and N intensity)		
	C	O	N
I	86.2	12.2	1.6
II	90.2	8.5	1.3
III	82.3	15.8	1.9
IV	90.3	8.7	1.0

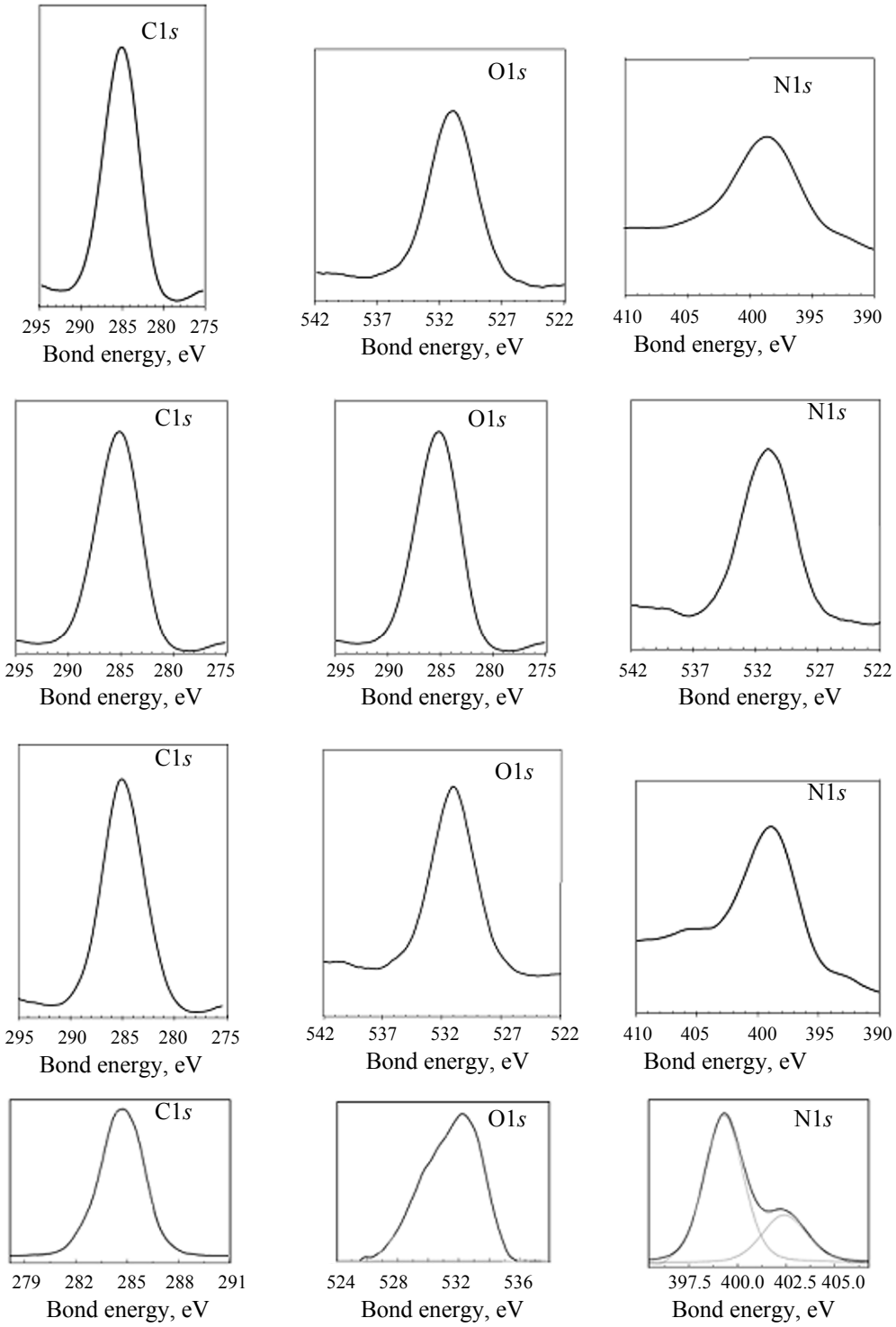

Fig. 6. X-ray photoelectron spectra of the initial nanodiamond samples I–IV.

Thus, the FTIR spectra are indicative of the presence of a set of different functional groups on the surface of all the diamond nanoparticles, with the difference in the nature of the carbonyl groups in the samples being the most pronounced.

The differences in the elemental composition of the diamond nanoparticle surface were confirmed by an XPS examination (Fig. 6 and Table 3). The highest oxygen and nitrogen content was found in samples I and III, which indicates that they have an oxidized

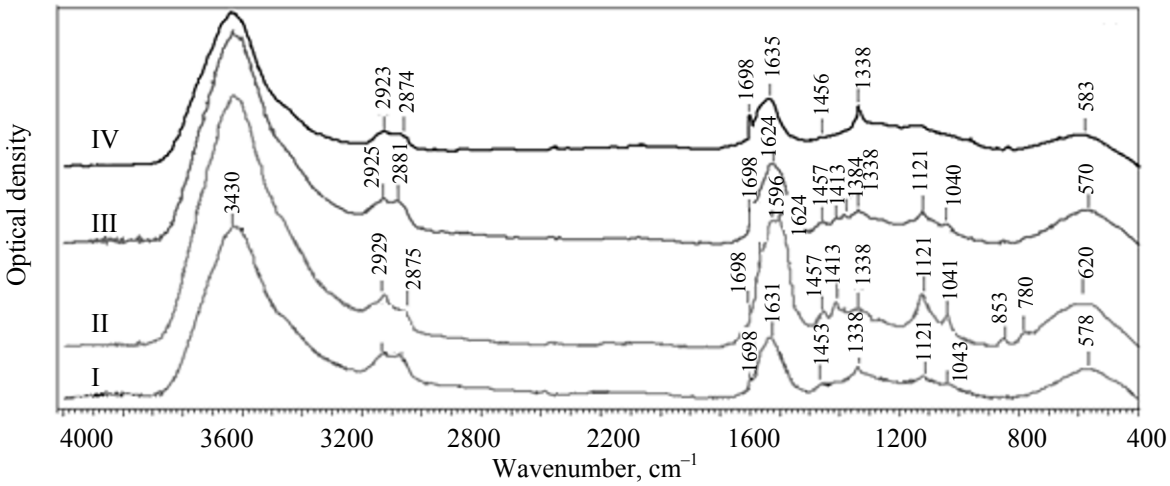

Fig. 7. FTIR absorption spectra of the hydrogenated nanodiamond samples.

surface. It should be noted that sample III is characterized by the highest oxygen content and, according to the producer, by the highest degree of deaggregation. In the XPS spectra, the N1*s* peak of sample IV is represented by two components, 399.3 and 402.5 eV. The latter component is associated with the presence of the NO_3^- ion whose vibrations were manifested in the FTIR spectrum of sample IV as an absorption maximum at 1384 cm^{-1}. This allows the former component (399.3 eV) to be assigned with certainty to the nitrogen in the composition of the nanodiamond particle proper [17].

The high-temperature heat treatment of the nanodiamond samples with hydrogen (800°C, 5 h) led to unification of the functional composition of the surface of all the samples, as demonstrated by Table 4 and Fig. 7. The FTIR spectra presented in Fig. 7 show that, after hydrogenation, the nanodiamond samples have identical surface compositions resulting from unification of their surface to –H and –OH groups. The hydrogenated nanodiamonds are able to form stable suspensions with aggregates of identical size (~50 nm), and the ζ-potential of the nanodiamond particles in the hydrosols ranges from 40 to 45 mV (see Table 2).

Table 4. Functional composition of the surface of the commercial nanodiamonds before and after hydrogen treatment according to the IR spectra

Wavenumber, cm^{-1}	Functional groups	Sample (initial/hydrogenated)			
		I	II	III	IV
1122	Ether, –C–O–C–	+ / +	+/ +	++/ ++	+/ +
1385	NO_3^-	+/ –	+/ –	+/ –	++++ / –
1630	Hydroxy	++++ / +++	+++ / ++++	++++ / +++	+++ /+++
1730	Carbonyl	– / –	+++/ –	–/ –	+/ –
1793	Bridging C–O–C	++ / –	+ / –	+++ / –	– / –
	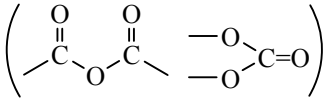				
2920–2880	H at sp^3 carbon atom	++ / +++	++ / +++	++ / +++	++ / +++
3430	Adsorbed water –OH	+++ / +++	+++ / +++	+++ / +++	+++ / +++

ACKNOWLEDGMENTS

This study was financially supported by the Russian Foundation for Basic Research (project nos. 11-03-00543 and 13-08-00647) and was carried out with the use of equipment purchased within the framework of the Lomonosov Moscow State University Development Program.

REFERENCES

1. Dolmatov, V.Yu., *Detonatsionnye nanoalmazy. Poluchenie, svoistva, primenenie* (Detonation Nanodiamonds: Preparation, Properties, and Application), St. Petersburg: Professional Research and Production Association, 2011.
2. El-Say, K.M., *J. Appl. Pharm. Sci*., 2012, vol. 1, no. 6, pp. 29–39.
3. Yakovlev, R.Yu, Solomatin, A.S., Leonidov, N.B., Kulakova, I.I., and Lisichkin, G.V., *Ross. Khim. Zh*., 2012, vol. 56, nos. 3–4, pp. 114–125.
4. Mazanov, V.A., *Phys. Solid State*, 2004, vol. 46, no. 4, pp. 629–635.
5. Danilenko, V.V., *Sintez i spekanie almaza vzryvom* (Synthesis and Sintering of Diamond by Explosion), Moscow: Energoatomizdat, 2003.
6. Kulakova, I.I., *Phys. Solid State*, vol. 46, no. 4, pp. 636–643.
7. Kulakova, I.I., in *Novye uglerodnye materialy: poluchenie, issledovanie, perspektivy primeneniya* (New Carbon Materials: Preparation, Research, and Application Prospects), Moscow: Nauka, 2013, pp. 44–62.
8. Kulakova, I.I., *Ross. Khim. Zh*., 2004, vol. 48, no. 5, pp. 97–106.
9. Bellamy, L.J., *The Infrared Spectra of Complex Molecules*, 2nd ed., New York: Wiley, 1966. Translated under the title *Novye dannye po IK-spektram slozhnykh molekul*, Moscow: Mir, 1970, p. 318.
10. Pretsch, E., Buhlmann, P., and Affolter, C., *Structure Determination of Organic Compounds: Tables of Spectral Data*, Berlin: Springer, 2000, p. 421.
11. Korobov, M.V., Avramenko, N.V., Bogachev, A.G., et al., *J. Phys. Chem*., 2007, vol. 111, pp. 7330–7334.
12. Korobov, M.V., Batuk, M.M., Avramenko, N.V., Ivanova, N.I., Rozhkova, N.N., and Ösawa, E., *Diamond Relat. Mater*., 2010, vol. 19, pp. 665–671.
13. Mochalin, V.N., Shenderova, O., Ho, D., and Gogotsi, Y., *Nat. Nanotechnol*., 2012, vol. 7, no. 1, pp. 11–23.
14. Man, H.B. and Ho, D., J. *Lab. Autom*., 2013, vol. 18, no. 1, pp. 12–18.
15. Fedutik, Yu.A., Antipov, A.A., Maltseva, E.A., et al., Abstracts of Papers, *3 Int. Symp. "Detonation Nanodiamonds: Technology, Properties, Applications,"* St. Petersburg, 2008, pp. 65–72.
16. Kurdyumov, A.V., Malogolovets, V.G., Novikov, N.V., et al., *Polimorfnye modifikatsii ugleroda i nitrida bora: Spravochnik* (The Polymorphs of Carbon and Boron Nitride: A Reference Book), Moscow: Metallurgiya, 1994, p. 200.
17. Kulakova, I.I., Korol'kov, V.V., Yakovlev, R.Yu., and Lisichkin, G.V., *Nanotech. in Russia,* 2010, vol. 5, nos. 7–8, pp. 474–485.